Available online at www.sciencedirect.com
SCIENCE DIRECT
Biochimica et Biophysica Acta 1758 (2006) 232–240
BIOCHIMICA ET BIOPHYSICA ACTA
BBA
http://www.elsevier.com/locate/bba

In situ characterization of lipid A interaction with antimicrobial peptides using surface X-ray scattering

Frances Neville [a], Chris S. Hodges [a], Chao Liu [b], Oleg Konovalov [c], David Gidalevitz [b,*]

[a] School of Process, Environmental and Materials Engineering, University of Leeds, Leeds LS2 9JT, UK
[b] Department of Chemical Engineering, Illinois Institute of Technology, 10 W. 33rd Street, R. 140, Chicago, IL 60616, USA
[c] European Synchrotron Radiation Facility, 6 Rue Jules Horowitz, BP 220, F-38043 Grenoble, Cedex, France

Received 15 December 2005; received in revised form 29 January 2006; accepted 31 January 2006

Abstract

Lipid A structure at the air–aqueous interface has been studied using pressure-area isotherm methods coupled with the surface X-ray scattering techniques of X-ray reflectivity (XR) and grazing incidence X-ray diffraction (GIXD). Lipid A monolayers were formed at the air–aqueous interface to represent the lipid moiety of the outer membrane of Gram-negative bacteria. Lipid A structure was characterized at surface pressures between 10 and 35 mN/m. Interactions of α-helical antimicrobial peptides LL-37, SMAP-29 and D2A22 with lipid A monolayers were subsequently studied. Although insertion into the lipid A monolayers was observed with the α-helical peptides, little change was seen from the X-ray data, suggesting that the lipid A hydrocarbon chains are involved in reorientation during insertion and that the hydrocarbon chains have a relatively rigid structure.
© 2006 Elsevier B.V. All rights reserved.

Keywords: Lipid A; Langmuir monolayer; Antimicrobial peptide; Lipopolysaccharide; GIXD; Reflectivity

1. Introduction

Microbial disease is on the increase worldwide [1–3] and because of this the development of novel antimicrobial pharmaceutical agents is of the utmost importance. In order for the design and development of new antibiotic drugs to progress, it is essential to understand how antimicrobial peptides kill bacteria.

The cell wall of Gram-negative bacteria is composed of two membranes, the outer membrane being composed of a phospholipid layer on the inner leaflet and a glycolipid layer on the outer leaflet. The glycolipid layer is composed of lipopolysaccharides (LPS) [4,5] and is anchored in place by the lipophilic moiety of the LPS known as lipid A [6,7]. Since lipid A is an important component of the outer membrane of Gram-negative bacteria, it is a prospective target for the design of novel antibacterial drug compounds. To this end, it is of interest to study its properties and the interactions between lipid A and other molecules.

The structure of lipid A can vary slightly depending on the bacterial species from which it is isolated [4]. Nevertheless, there has been a substantial body of work on the determination of the structure of lipid A isolated from *E. coli* [6,8–11]. It has been determined that lipid A (from *E. coli*) is a glucosamine disaccharide with β (1→6) linkage to two phosphate groups which are attached at positions 1 and 4′ [8,9]. Lipid A is also acylated, with up to seven acyl chains either amide- or ester-linked to the diglucosamine backbone [11]. The work carried out for this paper used a lipid A prepared from a rough strain (F583) of *E. coli* lipopolysaccharide. The naturally occurring cytotoxic diphosphoryl form of lipid A was used (Fig. 1).

Lipid A has previously been studied to observe its structural properties by using a range of techniques. Takayama et al. [7] combined mass spectrometry and NMR to study an early precursor in the biosynthesis of lipid A and postulated the structure of lipid A in *E. coli*. Imoto et al. [8] also used NMR to study the structure of the lipid A component of *E. coli* lipopolysaccharide and they later confirmed their results using

* Corresponding author. Tel.: +1 312 567 3534; fax: +1 312 567 8874.
E-mail address: gidalevitz@iit.edu (D. Gidalevitz).

0005-2736/$ - see front matter © 2006 Elsevier B.V. All rights reserved.
doi:10.1016/j.bbamem.2006.01.025

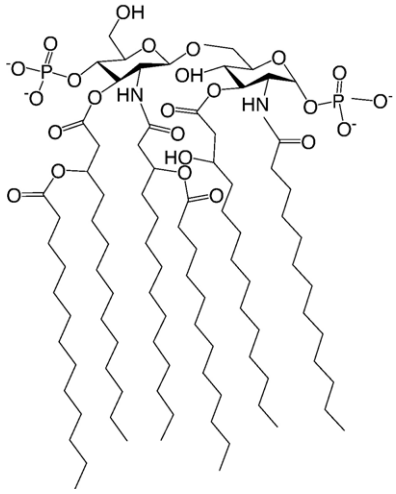

Fig. 1. Structure of lipid A molecule isolated from *E. coli*, with six hydrocarbon chains.

gas chromatography [9]. More recently, Seydel et al. [12] and Brandenburg et al. [11,13] used Fourier transform infrared (FTIR) spectroscopy to show that the tilt of different forms of lipid A varies with endotoxicity and that the comparison of a partial lipid A structure with a natural hexa-acyl lipid can be used to determine the biologically active unit of lipid A.

Lipid A is an essential part of the lipopolysaccharide and as such it can be used to study interactions of antimicrobial drug compounds with Gram-negative bacterial surfaces. One such type of antimicrobial agents which may be studied are antimicrobial peptides [14,15]. Antimicrobial peptides are of increasing interest for their potential as future pharmaceutical drugs since these peptides target the lipid regions of cell membranes and cause membrane disruption and cell death [15,16]. Antimicrobial peptides may be isolated from a variety of organisms and they are also being synthetically made. All the peptides used in this study come from the Cathelicidin family of peptides. LL-37 (LLGDFFRKSKEKIGKEFKRIVQRIKDFLRNLVPRTES) is the only human Cathelicidin antimicrobial peptide, SMAP-29 (RGLRRLGRKIAHGVKKYGPTVLRIIRIAG) is of ovine origin [17] and D2A22 (FARKFLKRFKKFVRKFIRFAFLF) is a designed synthetic analogue of a Cathelicidin peptide and it has bactericidal action against *S. aureus* and *P. aeruginosa* [18].

One of the most important stages of peptide–membrane interaction is the initial contact of the peptide with the outer leaflet of the membrane. In order to investigate how peptides interact with specific membrane lipids, methods that allow the membrane to be modeled in a fluid environment are needed. This may be carried out by the use of a Langmuir monolayer to mimic the external leaflet of the cell membrane, coupled with the introduction of peptides into the subphase of a Langmuir trough to represent the extracellular fluid and thus the approach of the peptide towards the cell surface. Langmuir monolayers of different lipids can be used to represent the membrane of different cell types and changes in membrane structure resulting from its interaction with peptides.

Lipid A structure and its interactions with other molecules was initially studied decades ago [6,7,9,10,19–21]. In recent years, research on lipid A structure at the air–aqueous interface and the interactions of lipid A with other molecules have become more prevalent [22–25]. Investigations of lipid A at the air–liquid interface utilizing Langmuir monolayers of lipid A molecules have been recently published [22,23,25]. It has been shown that both mono- and di-phosphoryl lipid A can form stable monolayers at the air–liquid interface which on compression show transitions from a liquid-expanded state to a more condensed one [22,23,25].

Some of this research focuses on interactions of lipid A films with antimicrobial peptides [22,25,26] and has observed these interactions with the use of the Langmuir trough technique coupled to other methods such as atomic force microscopy (AFM) [25], epifluorescence [26] and X-ray scattering [22]. The antimicrobial peptides studied with the lipid A systems include polymyxin B [25], protegrin-1 [22] and LL-37 [26]. The latter two publications presented for the first time compression and insertion isotherm data which showed phase transitions of lipid A at the aqueous surface and the changes in lipid A monolayer upon injection of peptides into the Langmuir trough subphase.

In this paper, a more detailed structural characterization of lipid A layers using surface X-ray scattering techniques is presented and structural studies of their interactions with antimicrobial peptides are attempted for the first time using grazing incidence X-ray diffraction and X-ray reflectivity techniques. Furthermore, these techniques are combined with insertion assays to observe the interaction of three different α-helical antimicrobial peptides.

2. Materials and methods

2.1. Lipid A monolayers

Lipid A is a major component of lipopolysaccharides from the outer layer of Gram-negative bacterial cell walls. Lipid A ([diphosphoryl, from *E. coli* F583], was purchased from Sigma-Aldrich and used without further purification. Lipid A was spread from a 74:23:3 v/v% chloroform: methanol:water solution.

2.2. Peptides

The peptides used in this study were synthetically made LL-37, SMAP-29 and D2A22. LL-37, SMAP-29 and D2A22 (90–95% purity) were purchased from Pepceuticals Ltd. A working solution of 10 μg/ml LL-37, SMAP-29 or D2A22 in 0.01% w/v acetic acid was injected under the subphase surface to give a final concentration in the subphase of 0.04 μg/ml or 0.1 μg/ml. All experiments were carried out with a subphase temperature of 22 °C±1 °C.

2.3. Pressure-area compression isotherms and pretreatment experiments

Insertion experiment data presented here were obtained using a custom-built trough [22,27] at the University of Chicago. All experiments were performed on Dulbecco's Phosphate Buffered Saline (DPBS) (Invitrogen Life Technologies) without calcium and magnesium ions. Pressure-area compression isotherms were carried out as follows. Upon spreading, the lipid A film was left undisturbed for 15 min to allow for solvent evaporation. At this point, barrier compression was initiated and the increase in surface pressure of the monolayer was monitored with decrease in area.

Pretreatment experiments were carried out to observe the extent of peptide self-assembly at the air–liquid interface when lipid A was present in

the gaseous phase and subsequently whether the peptide would remain incorporated in the lipid A layer at higher pressures if the peptide adsorbed at low pressure. A typical experiment consisted of lipid A being spread on the surface, the system being left to equilibrate (15 min) and subsequent peptide injection into the system under the lipid A monolayer using a microsyringe with a L-shaped needle (VDRL needle; Hamilton, Reno, NV). The data presented in this paper show pretreatment data for LL-37 and SMAP-29. After injection of peptide, the system was left for a further fifteen min in order to allow for any pressure changes due to injection of peptide to the system. The system was then compressed at a rate of 2 cm^2/min as for a normal pressure-area isotherm and the data compared with those of pure lipid A. Since the insertion assays involve compression of the lipid before peptide injection, these types of experiments have been termed "pretreatment" since the lipid layer is "pretreated" with the peptide before compression.

2.4. Insertion isotherms

Insertion experiments were carried out to quantify the interaction of antimicrobial peptides with the lipid A monolayer. Initially, the lipid A monolayer was deposited and equilibrated, followed by compression to the required surface pressure (ranging from 20 mN/m to 40 mN/m). This range of surface pressure was used as it corresponds to the liquid-condensed phase of lipids determined from repeated isotherms and the data would be able to be directly compared with data at the same pressures using different lipids [28]. Insertion isotherms were carried out in the constant pressure mode where the surface pressure was kept constant via a built-in controlled feedback system by adjusting the surface area. The peptide solution was then uniformly injected underneath the monolayer as in the pretreatment experiments. The injection of peptides under the compressed lipid monolayer mimics the approach by the peptide to the outer surface of the cell, as the hydrophilic head groups would be closest to the subphase, simulating the outer part of the membrane, and the peptide in the subphase would mimic the peptide in the extracellular fluid. The resulting relative change in area per molecule, $\Delta A/A$, was monitored throughout the experiment to compare the degree of peptide insertion into lipid A monolayers.

2.5. Grazing Incidence X-ray Diffraction (GIXD) and X-ray Reflectivity (XR)

X-ray scattering measurements were taken at the European Synchrotron Radiation Facility (ESRF), using a custom built Langmuir trough equipped with a single moveable barrier as described previously [22,28,29].

Grazing incidence X-ray diffraction (GIXD) [30] is used to obtain in-plane information concerning the molecular structure of surfaces [31]. For the GIXD measurements, the angle of incidence (α_i) was set to strike the air–aqueous interface at an incident angle of 0.8 α_c, where α_c is the critical angle for total external reflection. When the incident angle is less than the critical angle the phenomenon of total external reflection occurs and the refracted wave becomes an evanescent wave whose intensity decreases exponentially with depth and travels parallel to the interface below the surface. Typical penetration depth at 0.8 α_c is 76 Å. If the surface film contains order of a sufficiently long range, the evanescent wave will be diffracted by the ordered structure of the monolayer. This makes this method very surface sensitive. The intensity profile as a function of scattering angle was recorded by a linear position sensitive detector (PSD) that detected the diffracted beam. The incident wavelength used was 1.5 Å.

Grazing incidence X-ray diffraction measurements are made with variation of the X-ray momentum transfer component q_{xy} that is parallel to the air–aqueous interface. The reflections of the Bragg peaks observed with this geometry can be indexed by two Miller indices, hk. Their angular positions $2\theta_{hk}$, corresponding to $q_{hk}=(4\pi/\lambda)\ sin\ \theta_{hk}$, yield the repeat distances $d_{hk}=2\pi/q_{hk}=2\pi/q_{xy}$ for the two-dimensional (2D) lattice structure [32,33]. Bragg peak profiles (intensity against q_{xy}) were fitted with Gaussians and the peak position values were used to obtain unit cell dimensions of the lipid lattices. The observation of two Bragg peaks in the diffraction pattern of an amphiphilic monolayer is indicative of a distorted hexagonal (which can be viewed as centered rectangular) unit cell. Therefore, all unit cell dimensions in this paper have been calculated using the centered rectangular unit cell approximation.

Specular X-ray reflection measurements yield the gradient of electron density distribution perpendicular to the interface and may be used to model the film composition [30,32,34].

When specular X-ray reflection occurs, the scattering vector q_z (perpendicular to the surface) may be calculated from $q_z=4\pi \sin \alpha/\lambda$, where α is the grazing angle of the incident beam and λ the wavelength of the X-ray beam. When the reflectivity is measured as a function of the scattering vector q_z, the reflectivity curve contains information regarding the gradient of the electron density profile in the direction normal to the surface [33,35]. X-ray reflectivity measurements were carried out at a range of angles corresponding to q_z values of approximately 0 to 0.6 $Å^{-1}$. The reflected beam intensity was measured as a function of the incident angle using a PSD for simultaneous detection of specular reflection and diffuse scattering.

This provided an electron density profile averaged laterally across the footprint of the X-ray beam and was modeled by the deviation of the measured specular X-ray reflectivity from Fresnel's law for a perfect interface. The interface is modeled as a stack of slabs, where each slab has a constant electron density, thickness and interfacial roughness. The model was then least square fitted to the experimental data.

3. Results and discussion

3.1. Compression and pretreatment isotherms

The lipid A pressure-area isotherm (Fig. 2) has been measured all the way through until the monolayer collapsed at 60 mN/m. However, it is interesting to note that the area per molecule at 30 mN/m is approximately 127 $Å^2$/molecule. This is of interest for two main reasons. Firstly, the pressure corresponding to a lipid state in a natural membrane ranges from 25 to 40 mN/m [36–38] and thus it can be supposed that this is the approximate area per molecule lipid A would take within the membrane. Secondly, when comparing this value with other published work it can be seen that this value agrees with other published data [22,23,39] where the approximate area per molecule of lipid A is around 125–130 $Å^2$ in all three cases.

Although the lipid A molecule has an unusually complex structure for a membrane lipid (Fig. 1), its isotherm shows that the lipid A monolayer undergoes phase transitions on

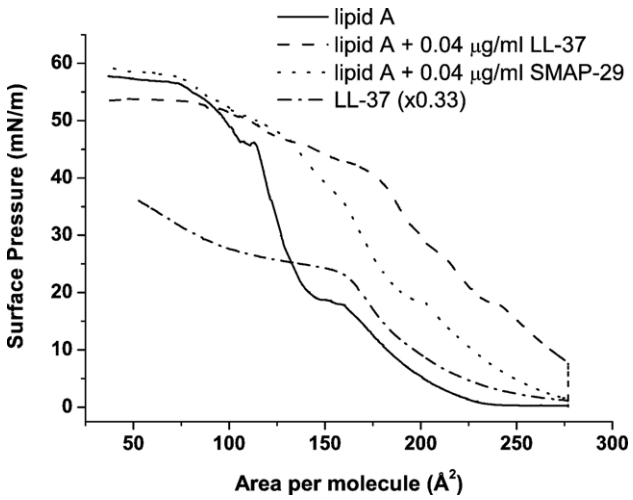

Fig. 2. Pure lipid A and pretreatment compression isotherms. LL-37 isotherm has been presented at a scale of one third of its real area per molecule, with the pressure values being those actually recorded. Area per molecule refers to area per lipid molecule.

compression as is observed with other phospholipids [22]. The compression pressure-area isotherm is qualitatively similar to others obtained previously [11,23,25]. However, the surface pressure value of the plateau region in the pressure-area isotherm (Fig. 2) is more comparable to the isotherm produced by Retzinger et al. [23] than to Brandenburg et al. [11] and the area per molecule values at the phase transition points are similar.

Pretreatment experiment data (Fig. 2) show there was an initial increase in pressure of approximately 8 mN/m when the LL-37 was injected under the lipid A film at ~0 mN/m, but there was much less increase with the SMAP-29 system. On compression, the lipid A liquid-extended/liquid-condensed phase transition is still visible in the both pretreated systems. However, it is shifted to the larger molecular area values by around 70 Å^2/molecule units from the value seen in the pure lipid A isotherm for the LL-37 system and ~30 Å^2/molecule units for the lipid A with SMAP-29 system. The phase transition observed in the LL-37 isotherm is also visible in the lipid A with LL-37 system pretreatment compression curve, suggesting the presence of LL-37 at the surface as well as the lipid A. The onset of collapse of the lipid A with LL-37 system begins at a much larger value of area per molecule than for the pure lipid A monolayer and it could be speculated that the LL-37 binds to lipid A to form a complex at the air–liquid interface as has been suggested for the DPPG with LL-37 system [28]. The lipid A with SMAP-29 system shows similar tendencies to the LL-37 system but to a lesser extent. The pretreatment isotherms strongly suggest that the lipid A at the surface has some role in the attraction of antimicrobial peptides to Gram-negative bacterial surfaces.

3.2. Insertion isotherms

Insertion assay data for lipid A experiments using two concentrations of LL-37 (0.04 μg/ml and 0.1 μg/ml) at constant pressures of 30 mN/m and 40 mN/m (Fig. 3) show varying results depending on the concentration and pressure used. The systems with lower concentration of LL-37 show increases in area of around 32% at both 30 mN/m and 40 mN/m. However, a very large increase in area (~166%), is seen on the injection of 0.1 μg/ml LL-37 under the lipid A monolayer at 30 mN/m, whereas there is less insertion at the higher pressure. This is very similar to the DPPG systems which show a 180% increase in area at the same conditions of LL-37 insertion [26,28]. The data suggest that because the lipid A is more closely packed at the higher pressure of 40 mN/m, less insertion can occur, unlike DPPG with LL-37 at 40 mN/m [28] or lipid A with protegrin-1 at 35 mN/m [22], where critical destabilization, followed by monolayer collapse takes place.

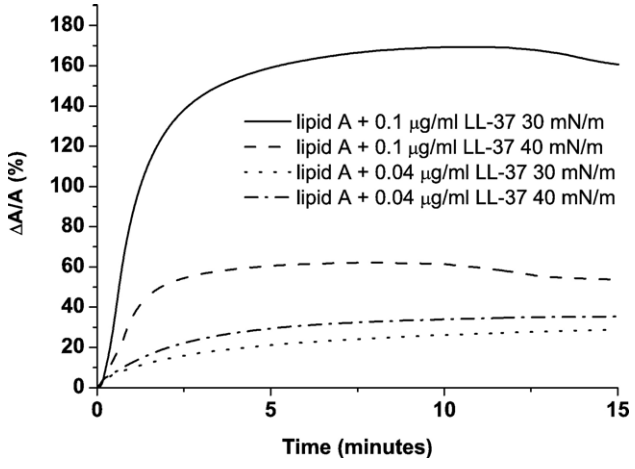

Fig. 3. Insertion isotherms of lipid A showing percentage change in area per molecule after injection of LL-37 at 30 mN/m and 40 mN/m constant pressure.

Insertion assays using SMAP-29 and D2A22 peptides at 30 mN/m and 40 mN/m (Fig. 4) show that the D2A22 and SMAP-29 peptides insert into the lipid A monolayer to a similar extent at 30 mN/m with an increase in area of around 40%. At the higher pressure of 40 mN/m, the SMAP-29 peptide inserts into the lipid A monolayer to a greater extent than the D2A22 peptide. This result may be attributed to differences in amino acid composition of these peptides. SMAP-29 has a higher overall net positive charge than D2A22 which could facilitate insertion. The high proportion of phenylalanine residues in D2A22 may contribute to the lower insertion seen at 40 mN/m, since the large proportion of bulky ring structures may inhibit penetration into the monolayer which is not the case with SMAP-29 as it only has one ring containing amino acid.

3.3. GIXD–Lipid A monolayers

Grazing incidence X-ray diffraction provides information on the in-plane structure of the lipid monolayer being studied. Lipid A has a much more complex structure (Fig. 1) than other membrane phospholipids such as phosphatidylcholine and phosphatidylglycerol lipids which only contain two hydrocarbon chains. Lipid A not only has a more complicated “head” group structure, but the tail groups, are more complex in structure. They can number up to seven per molecule due to the fact that the lipid is extracted from bacteria and therefore can contain lipid molecules which have not been fully synthesized in vivo. GIXD can be used in combination with pressure-area isotherms to determine the average structure of the lipid A molecules produced from the F583 strain of *E. coli.*

GIXD data (Fig. 5) of lipid A at 30 mN/m show two Bragg peaks with *d*-spacings of 4.33 Å and 4.19 Å, which correspond to centered rectangular unit cell dimensions of $a=5.06$ Å and $b=8.38$ Å and thus area per hydrocarbon chain of 21.2 Å^2. It is thought that the approximate area per molecule of lipid A at 30 mN/m is 120–130 Å^2 (Fig. 2) [11,22,23] thus demonstrating that there are on average six hydrocarbon chains per molecule. Therefore from the unit cell dimensions the area per molecule at 30 mN/m, the area per lipid A molecule is 127.2 Å^2. It is necessary to mention that due to the fact that the lipid is extracted from bacteria it contains a range of slightly different lipid A molecules (with varying numbers of hydrocarbon chains) and thus the exact molecular mass of lipid A cannot be determined and so the area per molecule has to be approximated to an average. Here, we have used a molecular mass of 1700 for lipid A as supplied by the manufacturer.

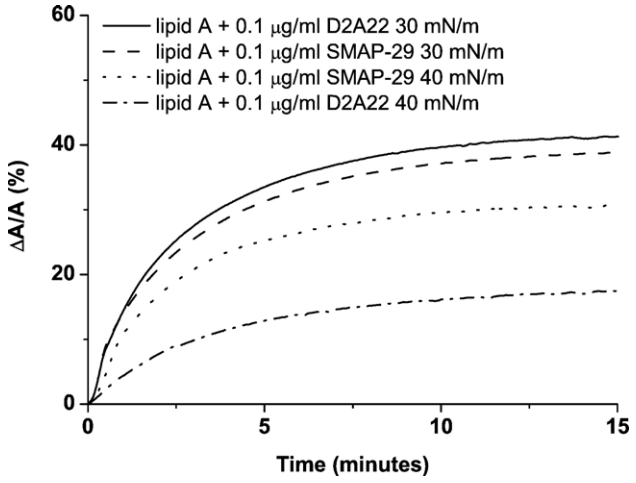

Fig. 4. Insertion isotherms of lipid A showing percentage change in area per molecule after injection of 0.1 μg/ml SMAP-29 and D2A22 at 30 and 40 mN/m [41].

The GIXD data of lipid A at 30 mN/m (Fig. 5) can be compared with the GIXD data of lipid A monolayers at 20 and 35 mN/m (data not shown). *d*-spacing values for the lipid A monolayer at 20 mN/m were determined as 4.37 Å and 4.15 Å, which translates to unit cell dimensions of $a=5.14$ Å and $b=8.30$ Å, which gives an area per unit cell of 42.7 Å^2 and an area per six hydrocarbon chain lipid A molecule of 128.1 Å^2. As expected, this value is slightly larger than that at 30 mN/m since the lipid A monolayer is less compressed than at 30 mN/m. The data of the lipid A monolayer at 35 mN/m gave *d*-spacing values of 4.31 Å and 4.17 Å, unit cell dimensions of $a=5.03$ Å and b 8.33 Å, with an area per lipid A molecule of 125.7 Å^2, assuming a lipid A molecule with an averaged number of hydrocarbon chains of six. This is smaller than at 20 and 30 mN/m as expected, due to further compression of the lipid A monolayer.

3.4. GIXD–Lipid A/peptide interactions

GIXD data of the lipid A monolayer at 30 mN/m after the injection of 0.04 μg/ml LL-37 as well as after injection of 0.1 μg/ml LL-37 [41] and SMAP-29 are shown in Fig. 5. GIXD results suggest that there is little apparent change to the tail order on addition of LL-37 or SMAP-29 to the system. However, the slight decrease in intensity suggests some peptide insertion, reducing the number of scattering centers from the ordered lipid A tail structure and thus the scattering intensity. For the lipid A with 0.04 μg/ml LL-37 system, the *d*-spacing values were 4.3 Å and 4.19 Å. This computes to unit cell dimensions of $a=5.06$ Å, $b=8.38$ Å and an area per molecule of $A=127.2$ Å^2 assuming a lipid A molecule with six hydrocarbon chains. The data for the higher concentration of LL-37 give *d*-spacing values of 4.32 Å and 4.19 Å, and unit cell dimensions of $a=5.05$ Å and $b=8.39$ Å, giving an area per molecule value of 127.2 Å^2 which is the same value as the lipid A monolayer alone and with the injection of the lower concentration of LL-37.

As can be seen from Fig. 5, the injection of SMAP-29 under the lipid A monolayer at 30 mN/m also gave very similar results to that of the pure lipid A monolayer. *d*-spacing values were 4.32 Å and 4.19 Å which gives unit cell dimensions of $a=5.05$ Å and $b=8.38$ Å and an area per molecule value of 126.9 Å^2 assuming a six chain lipid A molecule. The GIXD results of the lipid A after LL-37 and SMAP-29 insertion (Fig. 5) show that there was little apparent change to the lipid packing when the peptide was injected into the subphase. However, it is known that the peptide inserts into the lipid A monolayer due to a change in area per molecule during a constant pressure experiment (Figs. 3 and 4). This is thought to be due to the complex structure of the lipid A tail groups which cannot change greatly with regard to *d*-spacing due to their packing and thus can only change due to rotation of the molecules where the hydrocarbon chains remain with the same *d*-spacings. Also, the range in number of possible hydrocarbon chains may also have an effect on these lipid–peptide interactions.

3.5. XR–Lipid A characterization

Lipid A films were studied over a range of surface pressures which are relevant to physiological conditions [37,38] and X-ray reflectivity was used to structurally characterize lipid A monolayers at the air–aqueous interface.

The lipid A reflectivity data (Fig. 6) were modeled as two slabs, one representing the hydrophobic hydrocarbon chains, and the other the hydrophilic head region which contains the diphosphorylated sugar groups.

X-ray reflectivity data analysis of the lipid A system at 10 mN/m yielded a tail group slab thickness of 10.9 Å with an electron density normalized to the substrate (0.337 eÅ^{-3})

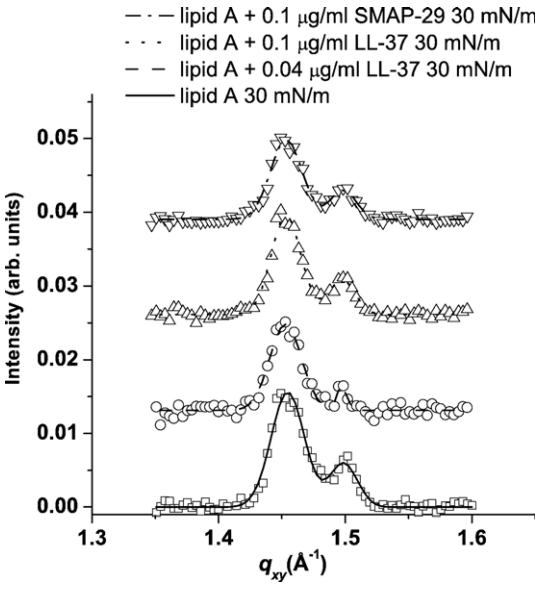

Fig. 5. Bragg peak plot of scattering vector q_{xy} as a function of intensity integrated over $q_z<1.1$ Å^{-1}—constant pressure experiments of injection of LL-37 or SMAP-29 under lipid A monolayer at 30 mN/m. The initial Bragg peaks from scattering of ordered structure of the lipid A monolayer are left practically unchanged on injection of LL-37 or SMAP-29 [41]. For clarity, the data have been offset vertically.

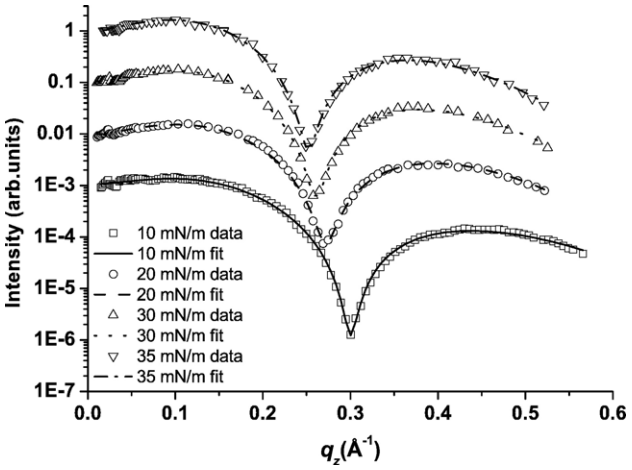

Fig. 6. X-ray reflectivity data and corresponding fits normalized by Fresnel reflectivity plotted against scattering vector (q_z) of lipid A monolayers at different pressures. The data show that the lipid A monolayer thickens on compression. For clarity, the data have been offset vertically.

of 0.97. The head group slab thickness was found to be 3.7 Å, with a normalized electron density of 1.57. The thickness of the tail group and its electron density can be attributed to the fact that the lipid A film is not tightly packed at this pressure (Fig. 2), and thus the tails of the lipid A molecules are not fully aligned or in an ordered structure. This is corroborated by the lack of Bragg peaks from the lipid A monolayer at 10 mN/m (data not shown). The electron density values may be calculated using the layer thickness and area per molecule at 10 mN/m (180 Å^2) to obtain the volume, when the number of electrons is known (assuming a hexa-acyl lipid A molecule). The calculated normalized electron density values are 0.95 and 1.57 for the tail and head groups, respectively, which show that the fitted values are in good agreements with the theoretically calculated ones. The thickness of the head group seems small at this pressure. However, it is suggested that this is because at this pressure the head group is aligned parallel to the air–aqueous surface due to the larger amount of space available to the lipid A molecules at this pressure. Upon compression the lipid A molecules reorient themselves, so that their hydrocarbon tails tilt and align to form an ordered structure. This is demonstrated in a schematic cartoon of the lipid A films at increasing pressures (Fig. 8A) which shows the rearrangement of the lipid A molecules on compression.

XR data analysis of lipid A monolayer at 20 mN/m showed that the tail group thickens on compression and the electron density of both the head and tail group increases. At 20 mN/m, the best fit yielded a lipid A tail group thickness of 13.3 Å with a normalized electron density of 0.99 and a head group thickness of 5.1 with an electron density of 1.65. At 20 mN/m, the lipid A has been compressed to the liquid-condensed phase (Fig. 2). The noticeable change in electron density and thickening of the tail group slab may be attributable to the alignment of the lipid A molecules into an ordered structure representing the liquid-condensed phase of the lipid monolayer.

3.6. XR–lipid A–host-defence peptide interactions

XR data for pure lipid A monolayer may be a good reference point for further experiments which involve peptide/lipid interaction. Any difference between the pure lipid A data and the data taken after peptide injection may be attributed solely to the effect of peptides on the interface structure.

XR data for lipid A with LL-37 system look very similar to the pure lipid A data, although there are subtle changes in terms of electron density and layer thickness (Fig. 7). The layer thickness values returned for lipid A with 0.04 μg/ml LL-37 system are 13.9 Å and 6.9 Å for the tail and head groups, respectively, which are reasonably similar to the values for the pure lipid A monolayer. Comparison of normalized electron density values for the tail and head group layers (0.92 and 1.44, respectively) to those of the pure lipid A monolayer at the same pressure, yields a decrease of up to 20% in normalized electron density after addition of LL-37. The electron density of LL-37 is approximately 0.381 e$^-$/Å^3 [28], and the normalized electron density of pure lipid A head group varies from 1.57 to 1.75. Therefore, the decreased electron density value of the lipid A film after LL-37 injection could be attributed to the fact that the LL-37 inserts mainly into the head region of the lipid A monolayer. Thus, the head group normalized electron density decreases from 1.75 to 1.44 whilst at the same time overall interfacial layer thickness increases because the peptides do not insert completely into the monolayer and some residues remain 'sticking out' into the subphase. The decrease in tail electron density can be explained accordingly. LL-37, inserting between lipid A head groups pushes apart the otherwise rigid lipid A molecules and thus the hydrocarbon chains of the lipid A molecules remain with the same number of electrons but occupy a greater area.

When the higher concentration of LL-37 peptide was used, a further change in the layer composition has been observed. The tail layer decreased in thickness to a value of 12.4 Å, with a

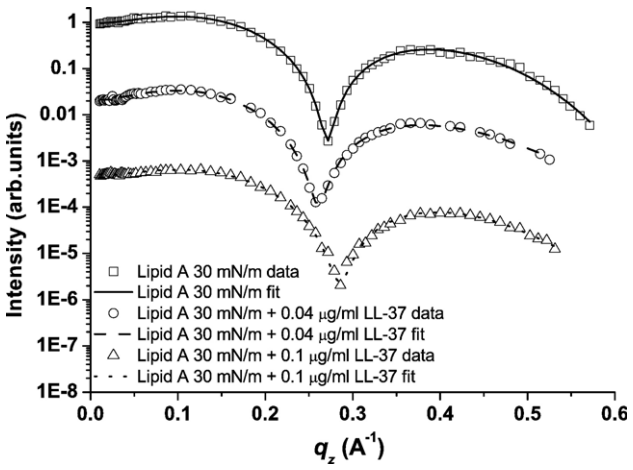

Fig. 7. Reflectivity data and corresponding fits of lipid A monolayer at 30 mN/m with injection of LL-37. The modeled fitting data show that there is a slight increase in lipid A layer thickness after addition of LL-37 due to insertion into the head group regions localized on the subphase side of the lipid A monolayer. For clarity, the data have been offset vertically.

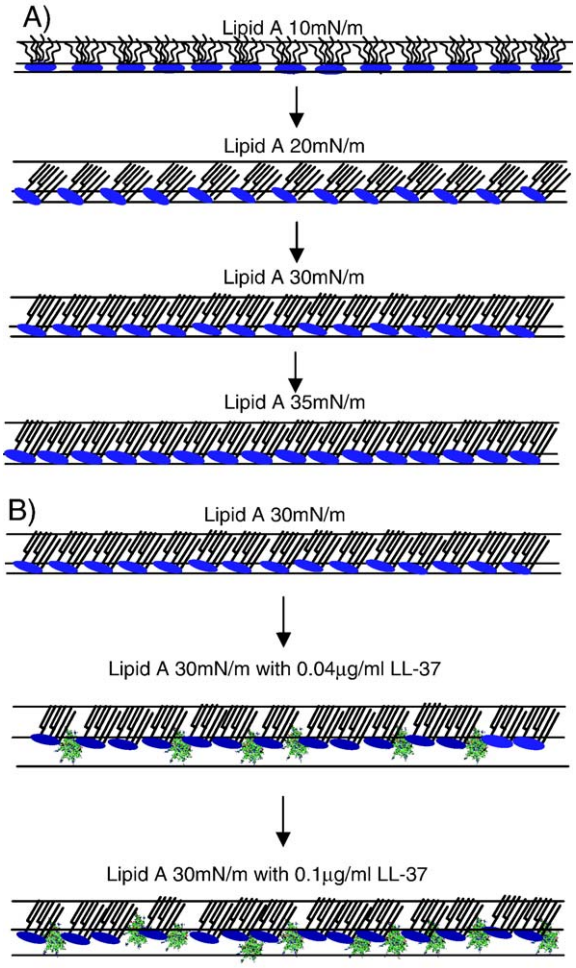

Fig. 8. Cartoon schematic of characterization of lipid A films at the air–aqueous interface and the possible interactions of LL-37 with lipid A monolayers.

normalized electron density of 0.98, and the head group further increased in thickness to a value of 8.5 Å, whilst decreasing in density to 1.32. This suggests that as more LL-37 is injected into the subphase, more peptides insert into the monolayer, which is corroborated by the insertion isotherms (Fig. 3).

A cartoon schematic of the interactions of LL-37 with lipid A monolayers is proposed (Fig. 8B). As has been previously discussed, it is thought that the tail structure of the lipid A molecules is fairly rigid and therefore it is more likely that the peptide will insert mostly into the head region of the lipid. When the concentration was increased from 0.04 μg/ml to 0.1 μg/ml, more peptide molecules inserted into the lipid A monolayer, exerting some pressure on the lipid molecules. This is corroborated by the fact that little change in the GIXD spectrum was observed upon peptide injection, but the XR data differ significantly indicating the increasing head group layer thickness and decrease in its electron density (Fig. 8B).

4. Summary and conclusions

The lipid component of the outer leaflet of the outer membrane of Gram-negative bacteria such as Escherichia, Salmonella and Chlamydia is composed a lipid known as lipid A. It is this lipid A component that is most likely to be targeted by antimicrobial peptides. The Langmuir monolayer approach to modeling peptide- or protein–membrane interactions proved to provide information inaccessible by other methods. However, to date no structural study of lipid A Langmuir films has been performed using GIXD and XR. This paper provides a detailed structural investigation of lipid A monolayers as well as lipid A films interaction with three different antimicrobial peptides.

The results of this study show how lipid A monolayers may be characterized using Langmuir trough techniques coupled to the X-ray scattering techniques of grazing incidence X-ray diffraction and X-ray reflectivity. This study also shows for the first time how the α-helical peptides LL-37, SMAP-29 and D2A22 can bind and insert to lipid A monolayers. The results presented in this paper may be combined with those previously published [26,28] and concurrent work [40] to provide a fuller picture on the peptide–lipid interactions of these systems.

The pretreatment experiments indicated that LL-37 and SMAP-29 α-helical peptides are likely to bind to lipid A and form some kind of lipid–peptide complex as was observed previously with DPPG monolayers [28]. This complex is then compressed until collapse, demonstrating that there is some permanent binding between lipid A and the peptide.

Insertion assays showed similar trends for the all the α-helical peptides used. In general, the greatest increase in molecular area upon peptide injection was displayed with the higher concentration of α-helical peptide at (0.1 μg/ml) and the lower pressure of 30 mN/m. Concurrent work [40] shows that a β-sheet peptide (Protegrin-1) shows similar insertion profiles to its truncated version, PC-17 which shows that peptides align themselves the same way round for insertion and that the arginine and glycine residues at the amine and carboxyl termini of the PG-1 peptide are not essential for peptide–lipid binding.

Analysis of the GIXD data indicates that the lipid A monolayer has an ordered structure. Although the insertion assays show an increase in area per lipid molecule when α-helical peptides are injected underneath the lipid A monolayer, GIXD data analysis shows little change in the unit cell dimensions of the systems before and after insertion. One possible explanation for this could be that at the pressure of 30 mN/m, the lipid A molecules are packed so tightly, that they cannot be altered significantly even in the presence of injected peptide and so the insertion occurs by rotation of lipid A molecules. This results in the same *d*-spacings being observed and so no apparent difference is seen when the data are compared before and after injection. The constant pressure mode allows the simulation of the outer leaflet of a membrane bilayer as the area can change, but the pressure must be maintained to keep the packed structure of the system. This demonstrates the elasticity of the membrane which may move in order to keep the pressure of the cell and avoid cell disruption, although the pressure is limited to a certain value which in real life could be exceeded in extreme circumstances.

The lipid A X-ray reflectivity data show the differences in the monolayer structure at different surface pressures. It is clear that monolayer packing at 10 mN/m is somewhat different than the rest of the data. This is due to the fact that there is a phase

transition at ~18 mN/m and below this value the lipid A monolayer appears to be in the liquid-expanded phase, rather than the liquid-condensed phase which is present after this co-existence phase transition. The XR data also show that the lipid A monolayer increases in thickness on compression which has been observed with other lipid monolayers [29]. Monolayer thickness values produced by other research groups are consistent with those presented here [23,25].

Analysis of the X-ray reflectivity data for the lipid A system after LL-37 peptide injection suggest that an increase in the peptide concentration in the subphase leads to a thickening of the lipid head group region. It is thought that this happens due to the partial insertion of LL-37 into the lipid A monolayer, with some adsorption to the head groups of the lipid A molecules. The tail group region of the lipid A monolayer is fairly rigid and thus the peptides insert mainly into the head group region. However, it is likely that some LL-37 molecules insert at least partially into the tail group regions, which is corroborated by increase in their electron density.

In summary, this paper presents for the first time a detailed study of lipid A monolayers at the molecular level using surface X-ray scattering techniques. It also shows that Langmuir monolayers of lipid A molecules can be used to model the outer leaflet of the outer membrane of Gram-negative bacteria in a fluid environment where the injection of peptides into the subphase represents the approach of the peptides to the bacterial cell surface. The results show that lipid A has an ordered structure at the air–liquid interface at biological relevant pressures and that antimicrobial peptides interact with lipid A monolayers to different extent depending on the peptide type and structure. An understanding of how different antimicrobial peptides interact with bacterial membrane components is essential for the production of future pharmaceutical therapeutic agents in the ongoing battle against antibiotic-resistant bacterial disease.

Acknowledgments

We thank Jeff Keen and Deidre Devine for providing the peptides. We are indebted to Yuji Ishitsuka and Ka Yee Lee for their help with ESRF measurements. We also acknowledge the European Synchrotron Radiation Facility for provision of synchrotron radiation facilities at the ID10B beamline. This project is sponsored by the Engineering and Physical Sciences Research Council, UK and IIT Armour College of Engineering startup funding.

References

[1] A. Tonks, Drug resistance is a worldwide threat, warns report, BMJ 309 (1994) 1109.
[2] C.A. Hart, S. Kariuki, Antimicrobial resistance in developing countries, BMJ 317 (1998) 647–650.
[3] M.H. Reacher, A. Shah, D.M. Livermore, M.C.J. Wale, C. Graham, A.P. Johnson, H. Heine, M.A. Monnickendam, K.F. Barker, D. James, R.C. George, Bacteraemia and antibiotic resistance of its pathogens reported in England and Wales between 1990 and 1998: trend analysis, BMJ 320 (2000) 213–216.
[4] C.R.H. Raetz, Biochemistry of endotoxins, Annu. Rev. Biochem. 59 (1990) 129–170.
[5] K. Brandenburg, W. Richter, M.H.J. Koch, H.W. Meyer, U. Seydel, Characterization of the nonlamellar cubic and HII structures of lipid A from *Salmonella enterica* serovar Minnesota by X-ray diffraction and freeze-fracture electron microscopy, Chem. Phys. Lipids 91 (1998) 53–69.
[6] A.J. Burton, H.E. Carter, Purification and characterization of lipid a component of lipopolysaccharides from *Escherichia coli*, Biochem 3 (1964) 411–418.
[7] K. Takayama, N. Qureshi, P. Mascagni, M. Nashed, L. Anderson, C. Raetz, Fatty acyl derivatives of glucosamine 1-phosphate in *Escherichia coli* and their relation to lipid A. Complete structure of A diacyl GlcN-1-P found in a phosphatidylglycerol-deficient mutant, J. Biol. Chem. 258 (1983) 7379–7385.
[8] M. Imoto, S. Kusumoto, T. Shiba, H. Naoki, T. Iwashita, E.T. Rietschel, H. W. Wollenweber, C. Galanos, O. Luderitz, Chemical structure of *E. coli* lipid A: linkage site of acyl groups in the disaccharide backbone, Tetrahedron Lett. 24 (1983) 4017–4020.
[9] M. Imoto, S. Kusumoto, T. Shiba, E.T. Rietschel, C. Galanos, O. Luderitz, Chemical structure of *Escherichia coli* lipid A, Tetrahedron Lett. 26 (1985) 907–908.
[10] N. Qureshi, K. Takayama, P. Mascagni, J. Honovich, R. Wong, R. Cotter, Complete structural determination of lipopolysaccharide obtained from deep rough mutant of *Escherichia coli*. Purification by high performance liquid chromatography and direct analysis by plasma desorption mass spectrometry, J. Biol. Chem. 263 (1988) 11971–11976.
[11] K. Brandenburg, B. Lindner, A. Schromm, M.H.J. Koch, J. Bauer, A. Merkli, C. Zbaeren, J.G. Davies, U. Seydel, Physicochemical characteristics of triacyl lipid A partial structure OM-174 in relation to biological activity, Eur. J. Biochem. 267 (2000) 3370–3377.
[12] U. Seydel, M. Oikawa, K. Fukase, S. Kusumoto, K. Brandenburg, Intrinsic conformation of lipid A is responsible for agonistic and antagonistic activity, Eur. J. Biochem. 267 (2000) 3032–3039.
[13] K. Brandenburg, S. Kusumoto, U. Seydel, Conformational studies of synthetic lipid A analogues and partial structures by infrared spectroscopy, Biochim. Biophys. Acta 1329 (1997) 183–201.
[14] D. Andreu, L. Rivas, Animal antimicrobial peptides: an overview, Biopolymers 47 (1998) 415–433.
[15] M. Zasloff, Antimicrobial peptides of multicellular organisms, Nature 415 (2002) 389–395.
[16] R. Bals, J.M. Wilson, Cathelicidins—A family of multifunctional antimicrobial peptides, Cell. Mol. Life Sci. 60 (2003) 711–720.
[17] B.F. Tack, M.V. Sawai, W.R. Kearney, A.D. Robertson, M.A. Sherman, W. Wang, T. Hong, M.B. Lee, H. Wu, A.J. Waring, R.I. Lehrer, SMAP-29 has two LPS-binding sites and a central hinge, Eur. J. Biochem. 269 (2002) 1181–1189.
[18] U. Schwab, P. Gilligan, J. Jaynes, D. Henke, n Vitro activities of designed antimicrobial peptides against multidrug-resistant cystic fibrosis pathogens, Antimicrob. Agents Chemother. 43 (1999) 1435–1440.
[19] L. Rothfield, R.W. Horne, Reassociation of purified lipopolysaccharide and phospholipid of the bacterial cell envelope: electron microscopic and monolayer studies, J. Bacteriol. 93 (1967) 1705–1721.
[20] M. Ivanova, I. Panaiotov, T. Trifonova, M. Echenazi, G. Konstantinov, R. Ivanova, Interaction of antilipid A immunoglobulin G and normal immunoglobulin G, incorporated in a lipid A monolayer, Colloids Surf. 10 (1984) 269–282.
[21] M. Ivanova, I. Panaiotov, M. Eshkenazy, R. Tekelieva, R. Ivanova, Interaction of lipid A with antilipid A immunoglobulin G and normal immunoglobulin G in mixed monolayers, Colloids Surf. 17 (1986) 159–167.
[22] D. Gidalevitz, Y.J. Ishitsuka, A.S. Muresan, O. Konovalov, A.J. Waring, R.I. Lehrer, K.Y.C. Lee, Interaction of antimicrobial peptide protegrin with biomembranes, Proc. Natl. Acad. Sci. U. S. A. 100 (2003) 6302–6307.
[23] G.S. Retzinger, K. Takayama, Mitogenicity of a spread film of monophosphoryl lipid A, Exp. Mol. Pathol. 79 (2005) 161–167.

[24] V. Yamazaki, O. Sirenko, R.J. Schaefer, L. Nguyen, T. Gutsmann, L. Brade, J.T. Groves, Cell membrane array fabrication and assay technology, BMC Biotechnol. 5 (2005) 18–29.
[25] S. Roes, U. Seydel, T. Gutsmann, Probing the properties of lipopolysaccharide monolayers and their interaction with the antimicrobial peptide polymyxin B by atomic force microscopy, Langmuir 21 (2005) 6970–6978.
[26] F. Neville, M. Cahuzac, A. Nelson, D. Gidalevitz, The interaction of antimicrobial peptide LL-37 with artificial biomembranes: epifluorescence and impedance spectroscopy approach, J. Phys. Condens. Matter. 16 (2004) S2413–S2420.
[27] A. Gopal, K.Y.C. Lee, Morphology and collapse transitions in binary phospholipid monolayers, J. Phys. Chem., B 105 (2001) 10348–10354.
[28] F. Neville, M. Cahuzac, O. Konovalov, I. Ishitsuka, K.Y.C. Lee, G.M. Kale, D. Gidalevitz, Lipid head group discrimination by antimicrobial peptide LL-37: Insight into mechanism of action, Biophys. J. 90 (2006) 1275–1287.
[29] O. Konovalov, I. Myagkov, B. Struth, K. Lohner, Lipid discrimination in phospholipid monolayers by the antimicrobial frog skin peptide PGLa. A synchrotron X-ray grazing incidence and reflectivity study, Eur. Biophys. J. Biophys. Lett. 31 (2002) 428–437.
[30] J. Als-Nielsen, D. McMorrow, Elements of Modern X-ray Physics, John Wiley and Sons, Chichester, 2001.
[31] T.R. Jensen, K. Balashev, T. Bjornholm, K. Kjaer, Novel methods for studying lipids and lipases and their mutual interaction at interfaces: Part II. Surface sensitive synchrotron X-ray scattering, Biochimie 83 (2001) 399–408.
[32] M. Losche, Surface-sensitive X-ray and neutron scattering characterization of planar lipid model membranes and lipid/peptide interactions, Curr. Top. Membr. 52 (2002) 117–161.
[33] J. Als-Nielsen, D. Jacquemain, K. Kjaer, F. Leveiller, M. Lahav, L. Leiserowitz, Principles and applications of grazing incidence X-ray and neutron scattering from ordered molecular monolayers at the air–water interface, Phys. Rep. 246 (1994) 251–313.
[34] M. Schalke, M. Losche, Structural models of lipid surface monolayers from X-ray and neutron reflectivity measurements, Adv. Colloid Interface Sci. 88 (2000) 243–274.
[35] C.A. Helm, H. Mohwald, K. Kjaer, J. Als-Nielsen, Phospholipid monolayer density distribution perpendicular to the water–surface—A synchrotron X-ray reflectivity study, Europhys. Lett. 4 (1987) 697–703.
[36] A. Seelig, Local anesthetics and pressure: a comparison of dibucaine binding to lipid monolayers and bilayers, Biochim. Biophys. Acta 899 (1987) 196–204.
[37] D. Marsh, Lateral pressure in membranes, Biochim. Biophys. Acta 1286 (1996) 183–223.
[38] A. Giehl, T. Lemm, O. Bartelsen, K. Sandhoff, A. Blume, Interaction of the GM2-activator protein with phospholipid±ganglioside bilayer membranes and with monolayers at the air±water interface, Eur. J. Biochem. 261 (1999) 650–658.
[39] S. Fukuoka, K. Brandenburg, M. Müller, B. Lindner, M.H.J. Koch, U. Seydel, Physico-chemical analysis of lipid A fractions of lipopolysaccharide from *Erwinia carotovora* in relation to bioactivity, Biochim. Biophys. Acta 1510 (2001) 185–197.
[40] F. Neville, I. Ishitsuka, O. Konovalov, K.Y.C. Lee, A.J. Waring, R.I. Lehrer, D. Gidalevitz, Interaction of Protegrin-1 with lipid monolayers using X-ray scattering techniques, In Preparation.
[41] 0.04 μg/ml and 0.1 μg/ml refer to final concentrations of peptide in solution.